Map-Based Modeling of Turbulent Convection

Application of the One-Dimensional Turbulence Model to Planar and Spherical Geometries

Marten Klein[1], David O. Lignell[2] & Heiko Schmidt[1]

[1] Dept. of Numerical Fluid and Gas Dynamics, Brandenburg University of Technology (BTU) Cottbus-Senftenberg, Cottbus, Germany
[2] Dept. of Chemical Engineering, Brigham Young University (BYU), Provo, UT

Brandenburg University of Technology Cottbus - Senftenberg

Introduction

Turbulent convection denotes the chaotic flow driven by buoyancy forces due to an unstable temperature stratification. The induced flow strongly affects the momentum and heat transfer between the bulk of fluid and the wall. An understanding of convecting flows is therefore relevant for many applications ranging from the technological to the geophysical context (e.g. [1] and references therein).

Turbulent convection has been studied numerically in planar and spherical geometries, where direct numerical simulations (DNSs) have reached the Rayleigh number $Ra = 2\times 10^{12}$ in 3-D [2] and $Ra = 10^{14}$ in 2-D [3]. Such simulations are extremely costly and in the case of long-time simulations constrained to $Ra \lesssim 10^{10}$ [1, 4]. Accurate and efficient modeling strategies are therefore needed if one wishes to increase the accessible range of Ra within the considerable future. For this objective, we suggest the map-based, so-called one-dimensional turbulence (ODT), modeling approach [5, 6]. We have extended the ODT formulation and present key results for planar and spherical convection cells.

Configuration

Rayleigh–Bénard (RB) setups considered in this study are shown in Fig. 1. The planar one is given by a fluid-filled cylinder with a heated bottom and cooled top with constant gravity g pointing downwards. For geophysical applications it can be crucial to take the spherical confinement geometry into account. Gravity $g(r)$ is directed in radial direction and its strength may vary with distance r from the center.

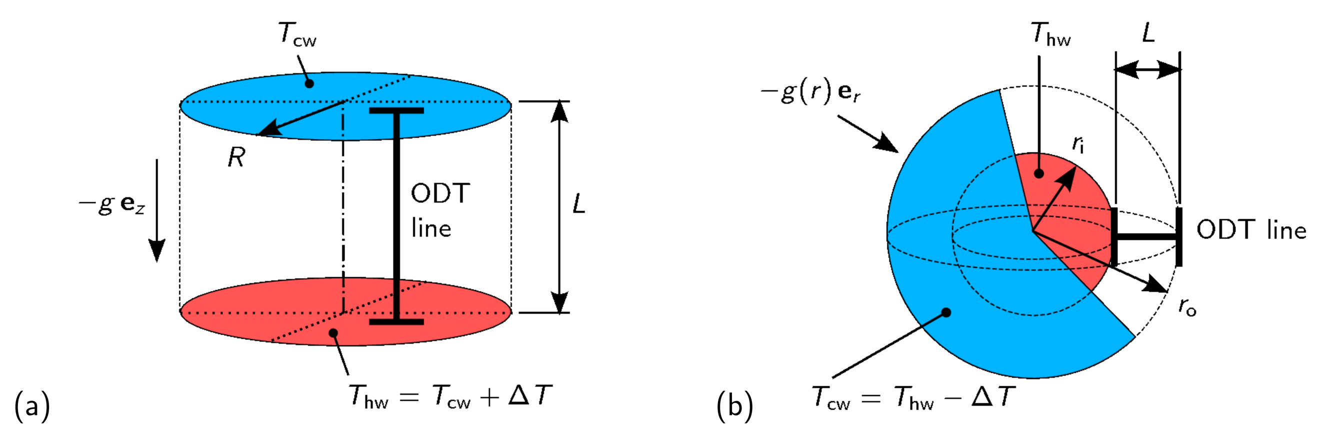

Figure 1: Schematic showing a planar (a) and spherical (b) Rayleigh–Bénard setup.

A convective flow in a given geometry is characterized by the Rayleigh and the Prandtl number,

$$Ra = \frac{g_0\,\beta\,\Delta T\,L^3}{\nu\kappa} \qquad \text{and} \qquad Pr = \frac{\nu}{\kappa},$$

where g_0 is the reference gravity, $\Delta T = T_{hw} - T_{cw}$ is the imposed temperature difference, L is the distance between the walls, β is the thermal expansion coefficient of the fluid, ν its kinematic viscosity, and κ its thermal diffusivity. Practically relevant values of Ra encompass several orders of magnitude, $10^6 \lesssim Ra \lesssim 10^{27}$, whereas $Pr \simeq 1$ for many working fluids [1]. Note that we only consider the linearized equation of state, $\rho(T) = \rho_0\left[1 - \beta\,(T - T_0)\right]$, where ρ is the density and T is the temperature.

ODT in a Nutshell

ODT is a stochastic turbulence model that resolves all scales of a turbulent flow, but reduces its dimensionality [5]. The computational domain is the *ODT line* (Fig. 1), which is a representative line of the turbulent flow. Property profiles (e.g. of the temperature and velocity) are evolved on this line by molecular diffusion. This deterministic part is interrupted by stochastic mapping events, so-called *eddy events*, which mimic the effect of turbulent advection as shown in Figs. 2 and 3.

An eddy event is characterized by three random variables: eddy size, position, and time of occurrence. The *triplet map* (TM) induces fluid displacement in the eddy-size interval centered at a given position which results in a local steepening of property gradients [5]. In spherical geometry, the mapping is radial so that the mapping has to compensate the volumetric stretching factor r^2 to maintain conservation properties. Here, the TMB has been used for this purpose [7].

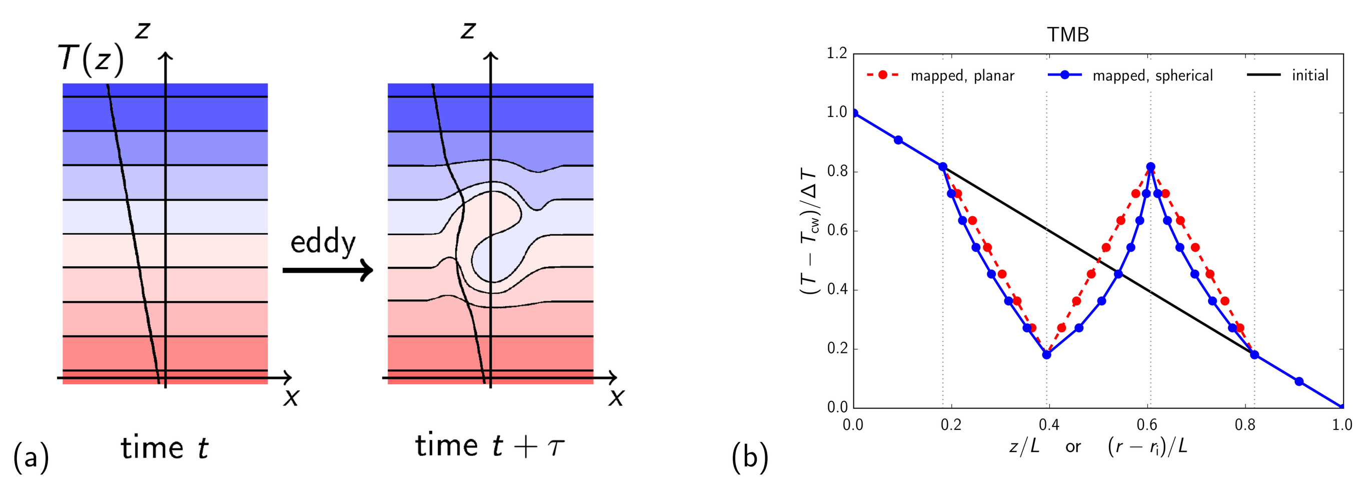

Figure 2: Schematic of an eddy turnover (a) and its 1-D representation due to the triplet map (b).

The random variables are sampled from guessed distributions so that the physical soundness of a candidate eddy event has to be tested with the momentary flow state [5]. The *eddy timescale* τ plays a central role in this respect and is given by [6, 7, 8]

$$\frac{1}{\tau} = \sqrt{\frac{2}{\rho_0 V l^2}\Big(\Delta E_{kin} + \Delta E_{pot} - Z\,E_{vp}\Big)} \qquad \text{so that} \qquad P_a = C\,\frac{\Delta t_s}{\tau},$$

where ΔE_{kin} and ΔE_{pot} denote the map-induced change of the kinetic and the potential energy, respectively, E_{vp} is the viscous penalty, V is the eddy volume ($V = l^3$ in planar geometry), P_a is the acceptance probability, and Δt_s is a time scale related to the sampling.

Numerical simulations have been performed with a fully-adaptive Langrangian finite-volume implementation of ODT [7, 9]. Representative ODT solutions are shown together with the corresponding sequence of eddy events in Fig. 3.

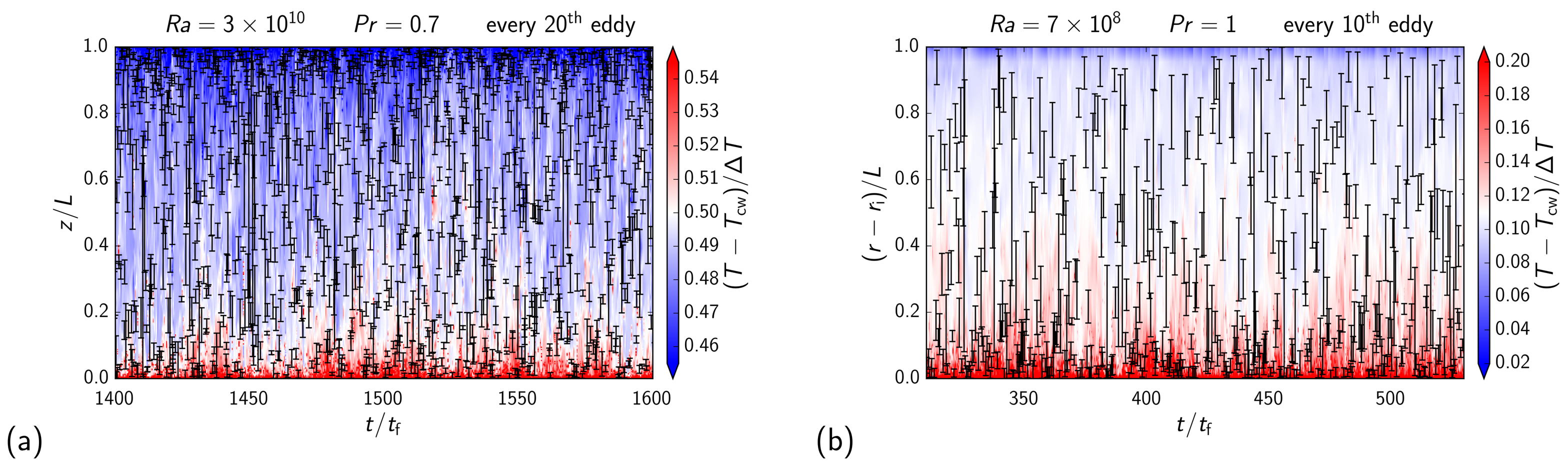

Figure 3: Space-time diagrams of ODT temperature solutions for planar (a) and spherical (b) geometry. Black lines mark implemented eddy events and $t_f = \sqrt{L/(g\,\beta\,\Delta T)}$ is the free-fall time.

Temperature and Velocity Profiles in Planar Geometry

The eddy-rate parameter C and the viscous-penalty parameter Z need to be determined with the aid of reference data for a given flow configuration. We optimized C and Z for planar RB cells by matching the mean wall-temperature gradient and the logarithmic region of the thermal boundary layer to reference data at $2\times10^{10} \le Ra \le 3\times10^{10}$ and $Pr = 0.7$ [2, 4]. This resulted in the optimal values $C = 60$ and $Z = 220$, which 'put' the ODT line on the axis of a cylindrical RB cell (Fig. 4). Other selections of model parameters are possible provided that $C(Z) \approx 4\sqrt{Z}$ [8]. A correlation between C and Z is also discussed in [6]. The local minimum in the fluctuations obtained with ODT is a known artifact [9].

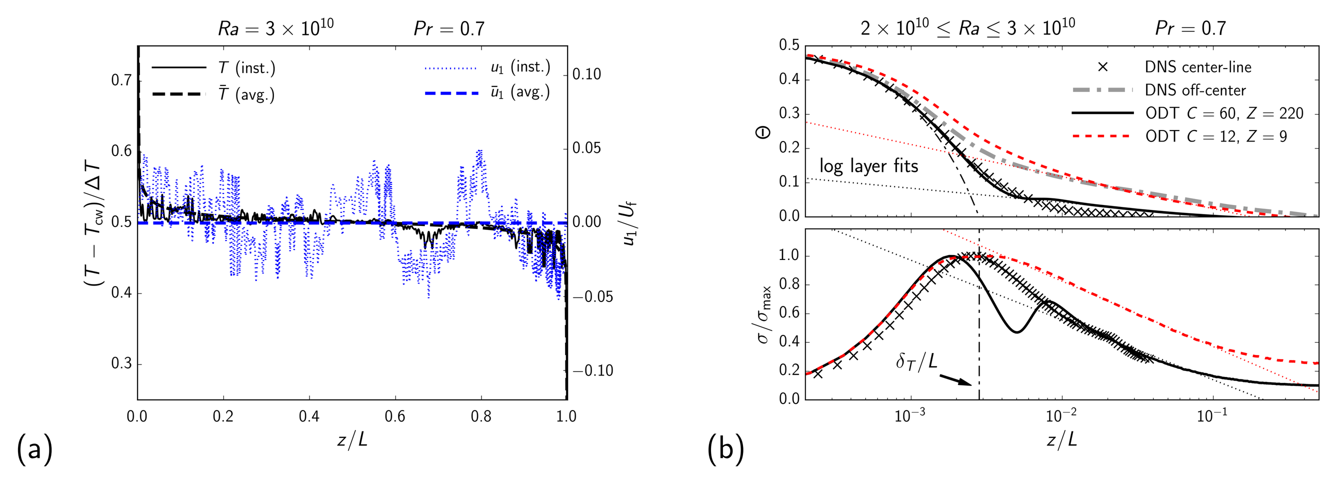

Figure 4: Profiles of the temperature T and the velocity u_1 normalized with the free-fall velocity $U_f = \sqrt{g\,\beta\,\Delta T\,L}$ are shown in linear scaling (a). Profiles of the normalized mean temperature $\Theta = (\bar{T} - T_m)/\Delta T$ with $T_m = (T_{hw} + T_{cw})/2$ (b, top) and of the standard deviation $\sigma = \sqrt{\overline{T^2} - \bar{T}^2}$ (b, bottom) are shown in semi-logarithmic scaling.

Temperature Profiles in Spherical Geometry

The radius ratio $\eta = r_i/r_o$ is a geometry parameter and appears automatically in the spherical ODT formulation [7], but inclusion of position-dependent gravity demands a model extension [8]. This is a modification of the planar formulation for uniform gravity [6].

In Fig. 5 the mean temperature profile of a slightly under-resolved DNS is compared with the corresponding ODT solution for which very good agreement has been obtained with the reference. To assess this further, the thermal boundary layer thickness $\delta_{T,i}$ at the inner sphere and $\delta_{T,o}$ at the outer one have been computed with the slope method. The asymmetry factor $\delta_{T,o}/\delta_{T,i}$ is expected to be independent of Ra for $Pr = 1$, but it will still depend on the ratio $g(r_i)/g(r_o)$ and η [10]. This is captured by ODT for $\eta \ge 0.25$ and all $g(r)$ investigated, but the asymmetry factor is systematically overestimated.

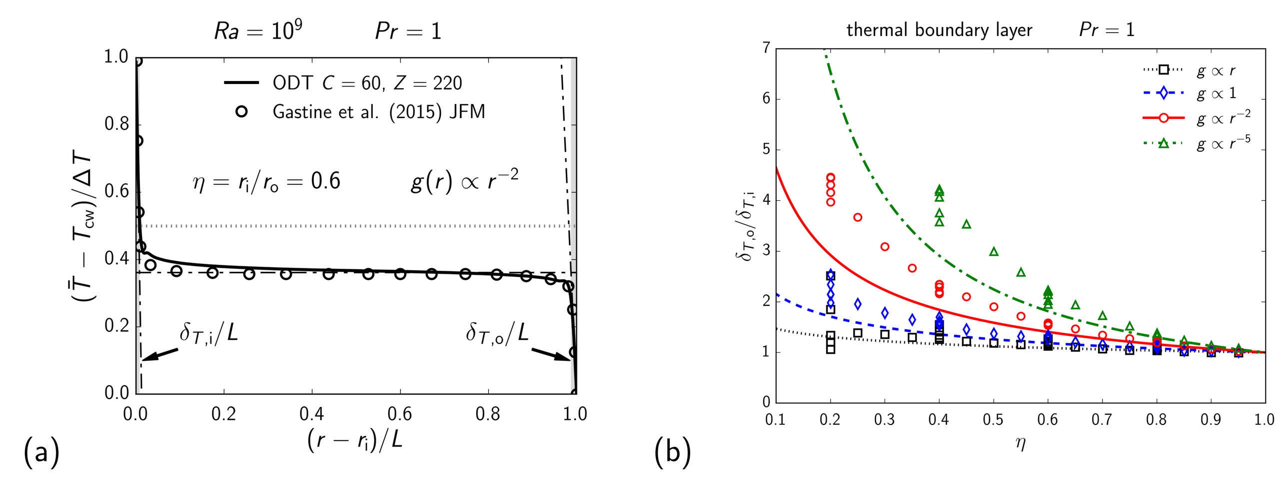

Figure 5: Radial profile of the mean temperature $\bar{T}$ (a). Asymmetry between the thermal boundary layer thickness at the outer and inner sphere in terms of the ratio $\delta_{T,o}/\delta_{T,i}$ for various Ra, η, and $g(r)$ (b).

Conclusions

- ODT formulation for spherical geometries and treatment of position-dependent gravity are validated.
- ODT is robust: One set of parameters gives reasonable results for Ra variation across 5 decades.
- Ra has to be large enough ($Ra > 10^8$) to make the assumption of structureless turbulence reasonable.
- The new eddy energetics can be useful for an application of ODT to Taylor–Couette flow (the flow between differentially rotating cylinders).

Forthcoming Research

- ODT simulations of the heat transfer up to $Ra \simeq 10^{17}$ (ultimate regime)
- Prandtl number variations

Acknowledgements

M.K. and H.S. acknowledge support by the German Academic Exchange Service (DAAD), which is funded by the Federal Ministry of Education and Research (BMBF), grant no. PPP-USA-2017, ID-57316240. M.K. also acknowledges support by the Graduate Research School (GRS) of the BTU Cottbus-Senftenberg in the form of mobility grants. Part of this work has been conducted in a project funded by the European Regional Development Fund (EFRE), grant no. StaF 23035000.

References

[1] F. Chillà and J. Schumacher. New Perspectives in Turbulent Rayleigh–Bénard Convection. *Eur. Phys. J. E*, 35:58, 2012.

[2] G. Ahlers, E. Bodenschatz, D. Funfschilling, S. Grossmann, X. He, D. Lohse, R. J. A. M. Stevens, and R. Verzicco. Logarithmic Temperature Profiles in Turbulent Rayleigh–Bénard Convection. *Phys. Rev. Lett.*, 109:114501, 2012.

[3] X. Zhu, V. Mathai, R. J. A. M. Stevens, R. Verzicco, and D. Lohse. Transition to the Ultimate Regime in Two-Dimensional Rayleigh-Bénard Convection. *Phys. Rev. Lett.*, 120:144502, Apr 2018.

[4] L. Li, N. Shi, R. du Puits, C. Resagk, J. Schumacher, and A. Thess. Boundary Layer Analysis in Turbulent Rayleigh–Bénard Convection in Air: Experiment versus Simulation. *Phys. Rev. E*, 86:026315, 2012.

[5] A. R. Kerstein. One-Dimensional Turbulence: Model Formulation and Application to Homogeneous Turbulence, Shear Flows, and Buoyant Stratified Flows. *J. Fluid Mech.*, 392:277–334, 1999.

[6] S. Wunsch and A. R. Kerstein. A Stochastic Model for High-Rayleigh-Number Convection. *J. Fluid Mech.*, 528:173–205, 2005.

[7] D. O. Lignell, V. Lansinger, J. Medina, M. Klein, A. R. Kerstein, H. Schmidt, M. Fistler, and M. Oevermann. One-Dimensional Turbulence Modeling for Cylindrical and Spherical Flows: Model Formulation and Application. Submitted to *Theor. Comp. Fluid Dyn.*, 2018.

[8] M. Klein, H. Schmidt, and D. O. Lignell. Map-Based Modeling of High-Rayleigh-Number Turbulent Convection in Planar and Spherical Confinements. In *Proc. Conference on Modelling Fluid Flow (CMFF'18)*, volume 0, pages 1–8, Budapest, Hungary, 2018. Accepted for publication.

[9] D. O. Lignell, A. R. Kerstein, G. Sun, and E. I. Monson. Mesh Adaption for Efficient Multiscale Implementation of One-Dimensional Turbulence. *Theor. Comp. Fluid Dyn.*, 27(3):273–295, 2013.

[10] T. Gastine, J. Wicht, and J. M. Aurnou. Turbulent Rayleigh–Bénard Convection in Spherical Shells. *J. Fluid Mech.*, 778:721–764, 2015.